Electronic Supplementary Information

Linker Engineering in Metal-Organic Frameworks for Dark Photocatalysis

Yating Pan,[‡a] Jingxue Wang,[‡a] Shengyi Chen,[b] Weijie Yang,[b] Chunmei Ding,[c] Amir Waseem,[d] and Hai-Long Jiang[*,a]

[a]Hefei National Laboratory for Physical Sciences at the Microscale, Department of Chemistry, University of Science and Technology of China Hefei, Anhui 230026, P. R. China

[b]School of Energy and Power Engineering, North China Electric Power University, Baoding 071003, P. R. China

[c]Dalian National Laboratory for Clean Energy, State Key Laboratory of Catalysis, Dalian Institute of Chemical Physics, Chinese Academy of Sciences, Dalian 116023, P. R. China

[d]Department of Chemistry, Quaid-i-Azam University, Islamabad 45320, I. R. Pakistan

[*]To whom correspondence should be addressed. E-mails: jianglab@ustc.edu.cn (H.-L.J)

[‡]These authors contributed equally to this work.

S1. Materials and Instruments

All chemicals were purchased from commercial sources and used without further purification. Powder X-ray diffraction patterns (XRD) were measured on a Japan RigakuMiniFlex 600 equipped with graphite-monochromated Cu Kα radiation (λ = 1.54178 Å). Fourier transform infrared (FTIR) spectra in 4000 to 400 cm^{-1} range were collected on a SHIMADZU IR Affinity-1 spectrometer with KBr discs. The ^{1}H nuclear magnetic resonance (^{1}HNMR, Bruker AVANCE AV III 400) spectroscopy was used to identify the functional group of ligands. Field-emission scanning electron microscopy (FE-SEM) with a field S3 emission scanning electron microanalyzer (Zeiss Supra 40 scanning electron microscope at 5 kV accelerated voltage) was carried out. UV-Vis absorption spectrum was obtained from Shimadzu UV-2700 spectrophotometer. The transmission electron microscopy (TEM) images were observed on a JEOL JEM-2100F field-emission transmission electron microscope. Zeta potential was investigated on Zeta potentiometer (DelsaNano C). Photoluminescence (PL) spectra (excitation at 250 nm) were measured with a PerkinElmer LS 55 fluorescence spectrophotometer in the solution of MeCN or MeCN contained with TEOA. Time-resolved photoluminescence spectra were taken on a FM4-2015 TCSPC transient fluorescence spectrometer. The catalytic reaction products were analyzed and identified by gas chromatography (Shimadzu GC-2014). The liquid products were analyzed using ion chromatography (CASTLE C1K-3K UPS). The consumption of TEOA was identified and analyzed by using a Shimadzu gas chromatograph (GC-2010 Plus with a 0.25 mm × 30 m Rtx-5 capillary column).

S2. Experimental Section

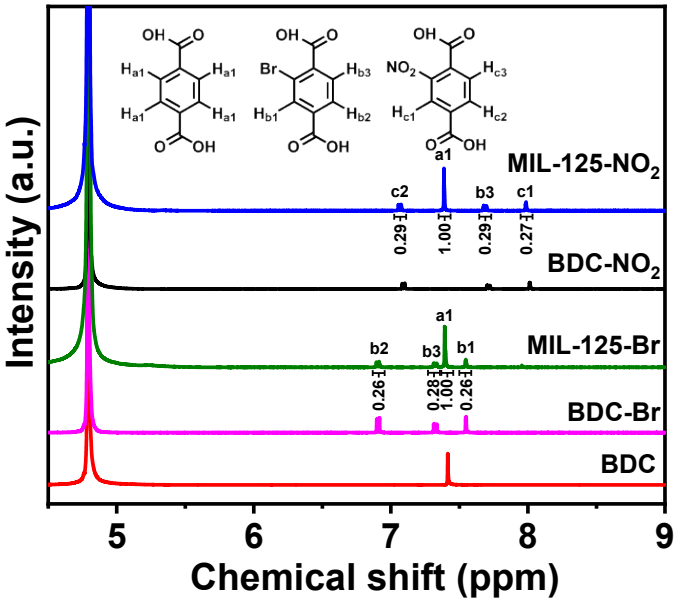

Fig. S1 ^{1}H NMR spectra of MIL-125-NO_2 and MIL-125-Br.

The maximum linker-exchange extent of MIL-125-NO_2 and MIL-125-Br is about 50% according to the peak area of different H of linkers in the above ^{1}H NMR spectra.

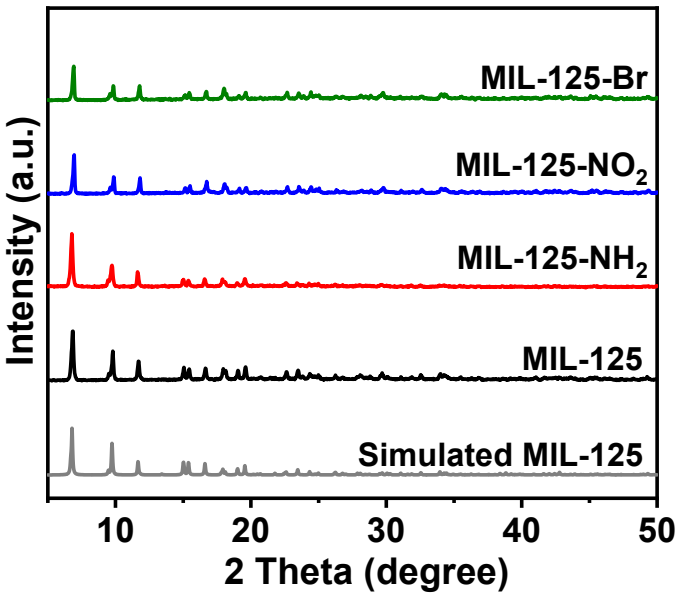

Fig. S2 Powder XRD patterns of MIL-125 and MIL-125-X (X = NH_2, NO_2, Br).

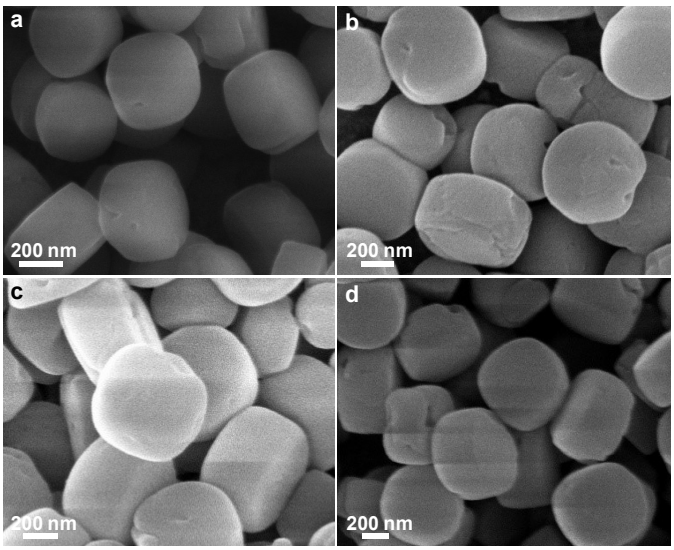

Fig. S3 SEM images of (a) MIL-125, (b) MIL-125-NH_2, (c) MIL-125-NO_2 and (d) MIL-125-Br.

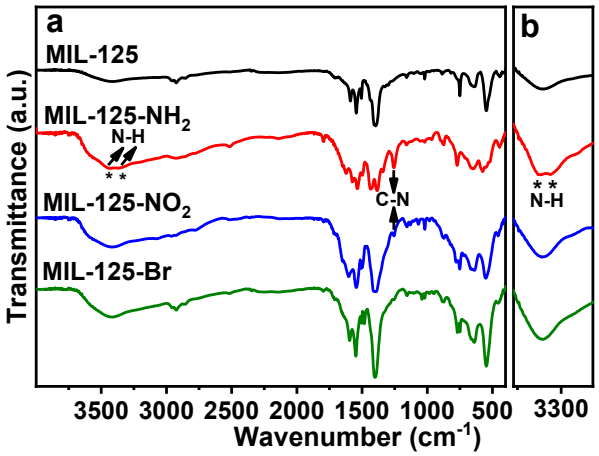

Fig. S4 (a) The FTIR spectra and (b) the enlarged FTIR spectra (3000 cm^{-1} to 3600 cm^{-1}) of MIL-125 and MIL-125-X (X = NH_2, NO_2, Br).

FTIR show peaks at 3351 cm^{-1} ($\nu_{sN\text{-}H}$), 3461 cm^{-1}($\nu_{asN\text{-}H}$), 1257 cm^{-1} ($\nu_{as\ C\text{-}N}$) and 550cm^{-1} ($\nu_{as\ C\text{-}Br}$),[S1] in which the $\nu_{as\ C\text{-}Br}$ is partially overlaid by a stretching vibration of Ti-O. Results suggest the successful introduction of different functional groups into MIL-125.

Fig. S5 The images of (a) MIL-125, (b) MIL-125-Br, (c) MIL-125-NO_2 and (d) MIL-125-NH_2.

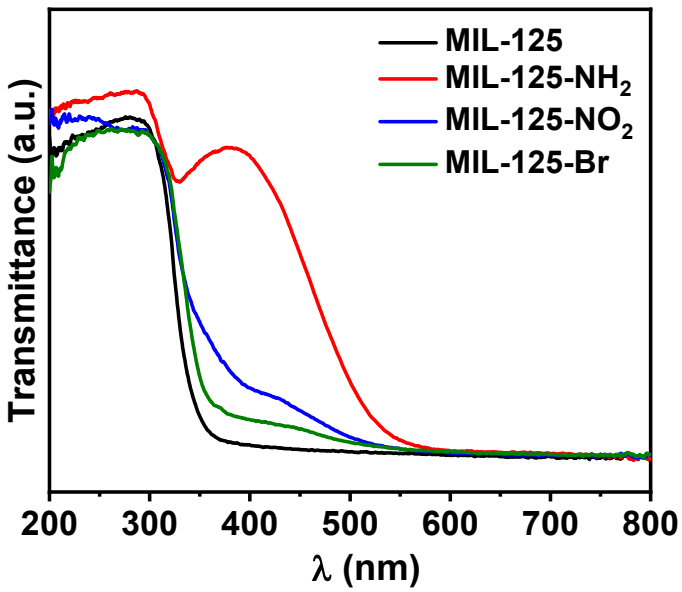

Fig. S6 UV-Vis absorption spectra of MIL-125 and MIL-125-X (X = NH_2, NO_2, Br).

The absorption band around 265 nm is induced by O to Ti charge transfer (LMCT = ligand-to-metal charge transfer) in the Ti-oxo clusters; the extended absorbance in the visible light region is assignable to the n-π* transition caused by the introduction of functional group.

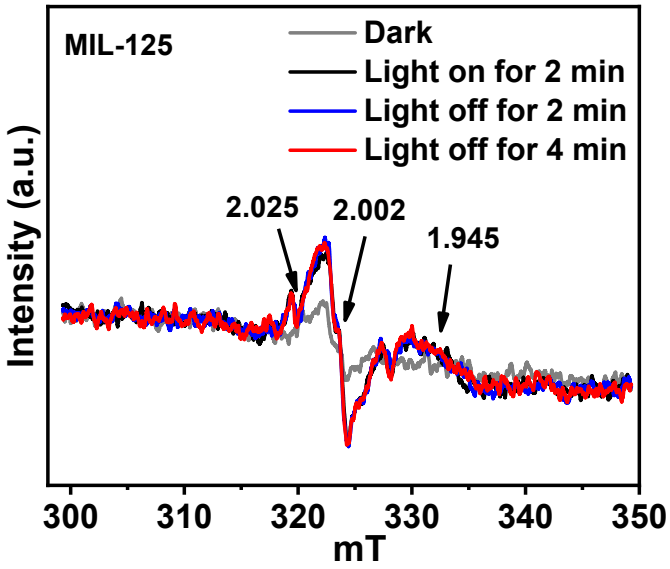

Fig. S7 The ESR spectra of MIL-125 in the dark, under light on and off for different time lengths.

Compared to MIL-125 in the dark, new EPR peaks at g = 1.945, 2.002 and 2.025 under light irradiation are assignable to the Ti^{3+} intermediates generated from the LMCT process and $O_2^{\bullet-}$ adsorbed onto Ti-oxo clusters (the residual O_2 molecules accept electrons from electron-trapped Ti-oxo cluster). Upon turning off the light, the EPR signal can be maintained for a long time, indicating the long-lived intermediate.

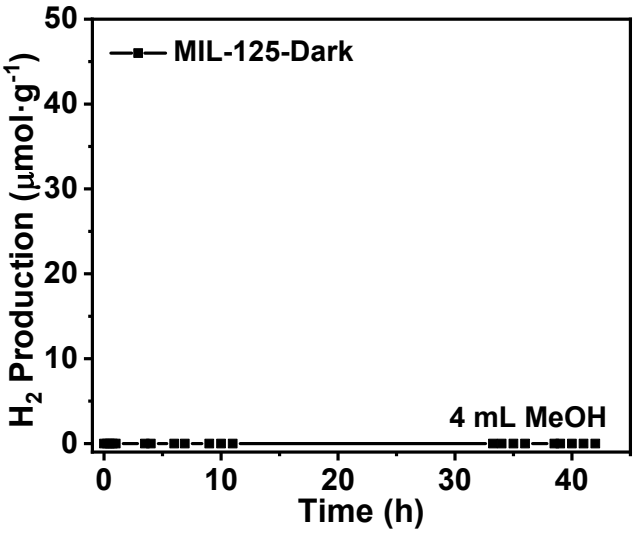

Fig. S8 The photocatalytic hydrogen production activity of MIL-125 in the presence of 4 mL MeOH under light off.

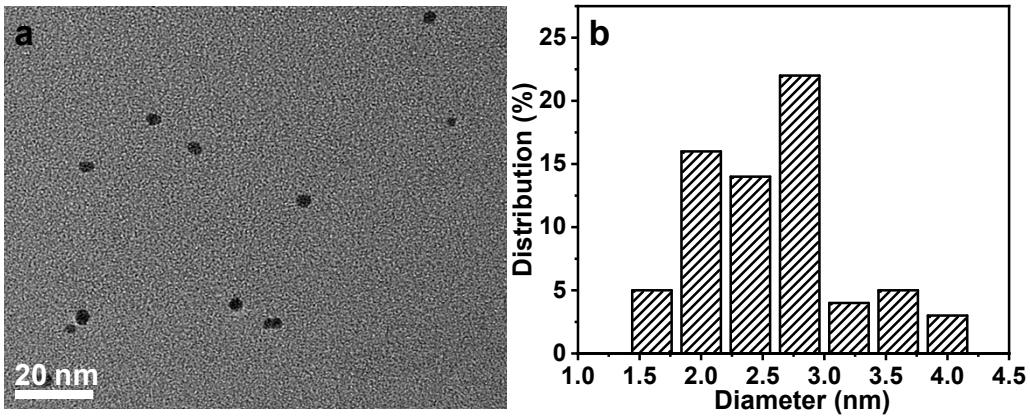

Fig. S9 (a) TEM image of Pt NPs and (b) the corresponding size distribution, indicating the Pt sizes are ~3 nm.

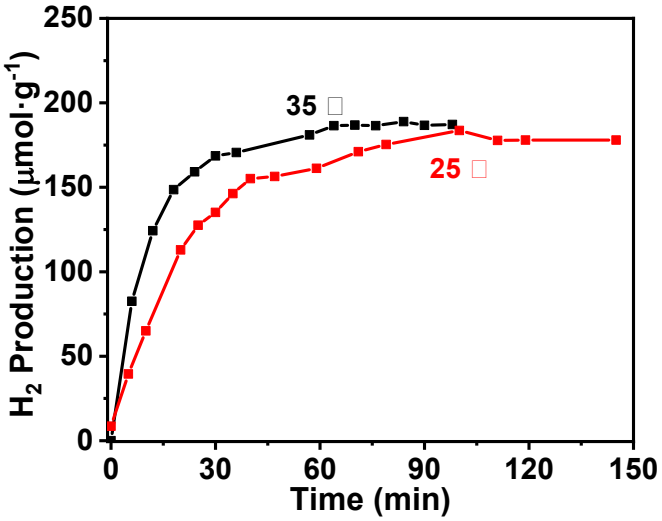

Fig. S10 The dark photocatalytic hydrogen production over MIL-125 in 2 mL MeOH with controlled reaction temperatures at 25 °C and 35 °C, respectively.

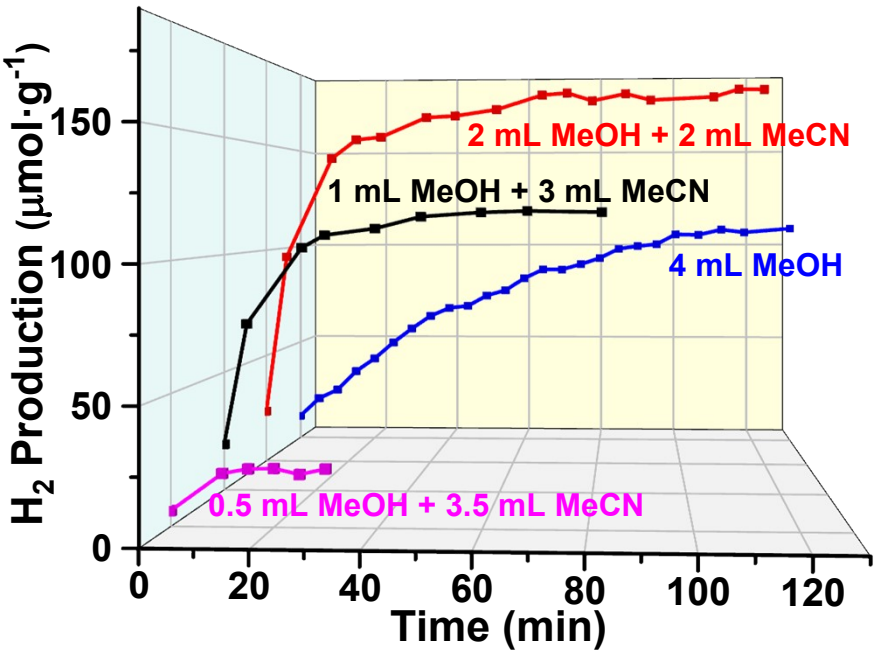

Fig. S11 The dark photocatalytic hydrogen production activity of MIL-125 in different concentrations of methanol sacrificial agent (MeOH) using acetonitrile as the solvent. The total solution volume was fixed to 4 mL. The reaction temperature is maintained at 25 °C.

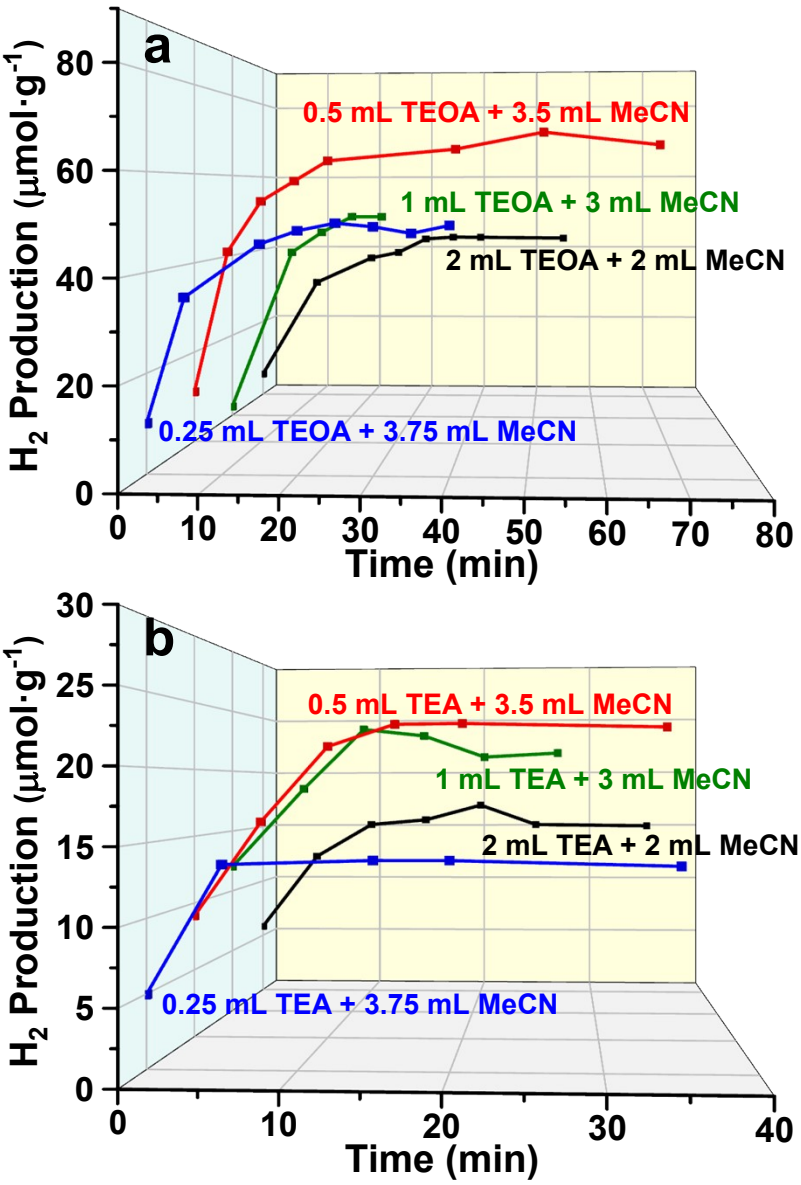

Fig. S12 The dark photocatalytic hydrogen production activity of MIL-125 in the presence of (a) TEOA or (b) TEA as a sacrificial agent in MeCN at 25 °C, by fixing the solution volume to 4 mL.

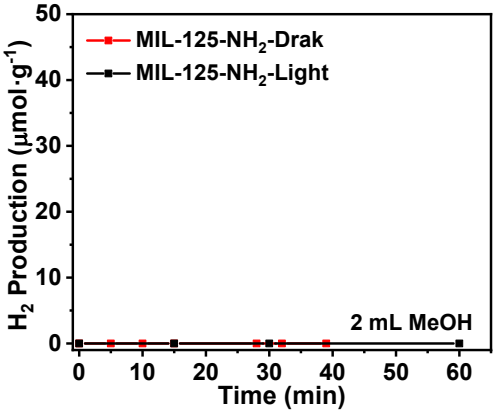

Fig. S13 The hydrogen production activity of MIL-125-NH_2 with 2 mL MeOH as a sacrificial agent and solution under dark and light irradiation at 25 °C.

MeOH is not a good sacrificial agent for MIL-125-NH_2. Accordingly, TEOA, which is efficient for hole removal of MIL-125-X (X = H, NH_2, NO_2, Br), is chosen as a sacrificial agent in our work to compare the role of different functional groups.

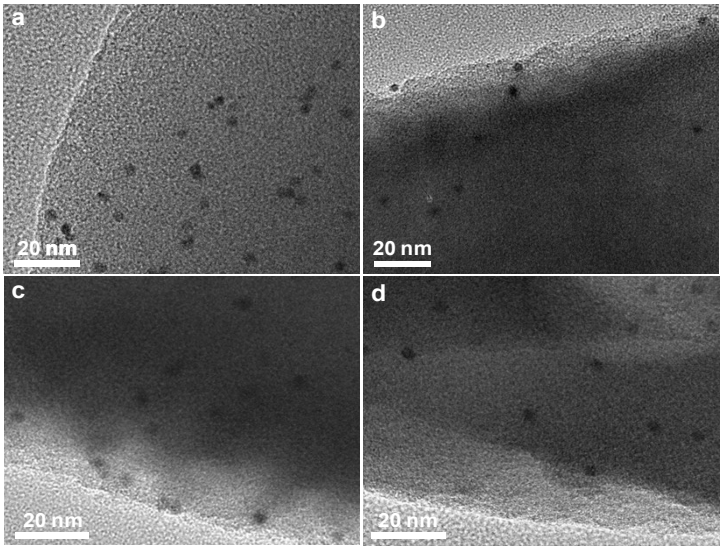

Fig. S14 The TEM images of (a) MIL-125, (b) MIL-125-NH_2, (c) MIL-125-Br, and (d) MIL-125-NO_2 after reaction.

The TEM images show that Pt NPs with similar sizes of 3 nm are evenly distributed on the isoreticular MOF surfaces. The dispersion of Pt is similar in different MOFs.

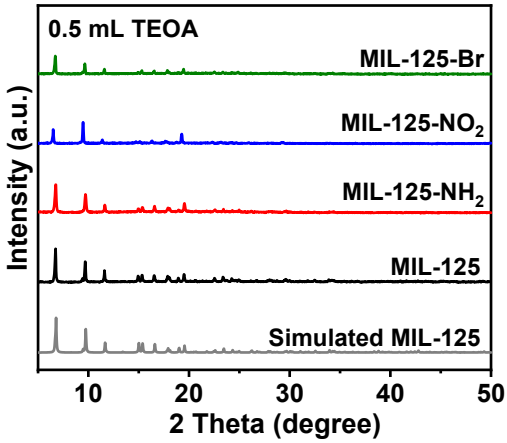

Fig. S15 Powder XRD patterns of MIL-125 and MIL-125-X (X = NH_2, NO_2, Br) after photocatalytic reaction, suggesting their maintained crystallinity.

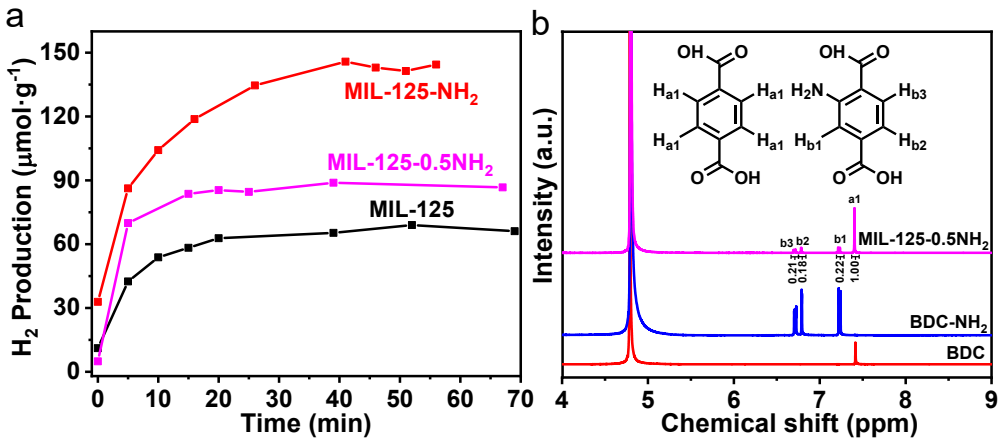

Fig. S16 (a) The dark photocatalytic hydrogen production activity comparison of MIL-125, MIL-125-NH_2 and MIL-125-0.5NH_2 with TEOA as a sacrificial agent at 25 °C. (b) ^{1}H NMR spectra of MIL-125-0.5NH_2, BDC-NH_2 and BDC.

The higher dark photocatalytic activity of MIL-125-0.5NH_2 than MIL-125 is in line with the overall activity trend, indicating that the introduction of -NH_2 group is conducive to the improvement of dark reaction activity.

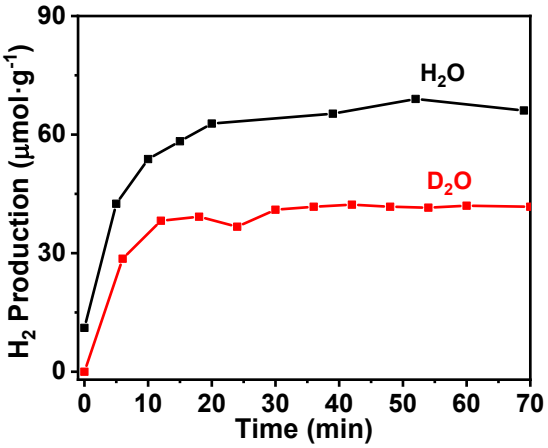

Fig. S17 The dark photocatalytic hydrogen production activity of MIL-125 in MeCN with TEOA as a sacrificial agent at 25 °C, in the presence of H_2O and D_2O as a hydrogen source, respectively.

The experiment with D_2O gives reduced hydrogen production activity due to the difficult bond cleavage of D-O, indicating that the H source is from water, as concluded by the previous report.[S2]

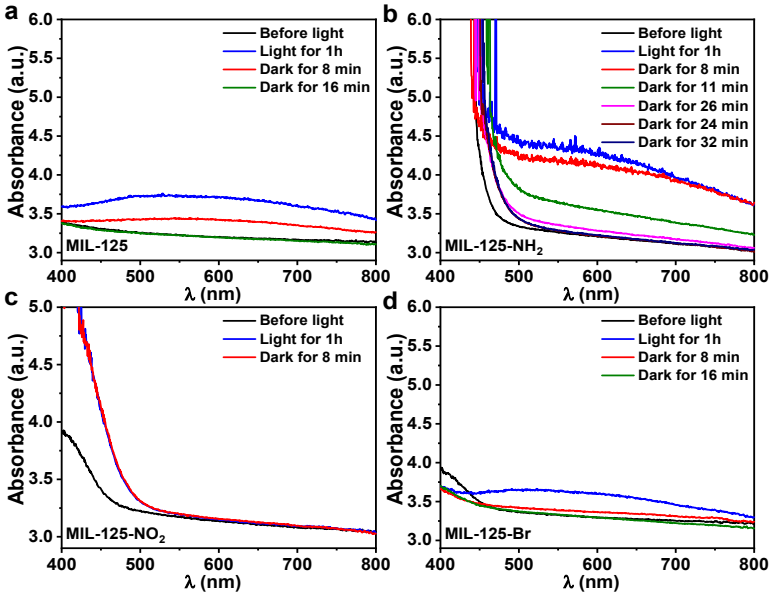

Fig. S18 The vacuum liquid UV-Vis absorption spectra of (a) MIL-125, (b) MIL-125-NH_2, (c) MIL-125-NO_2 and (d) MIL-125-Br before light on and after light on/off for different time lengths in MeCN with TEOA as sacrificial agent.

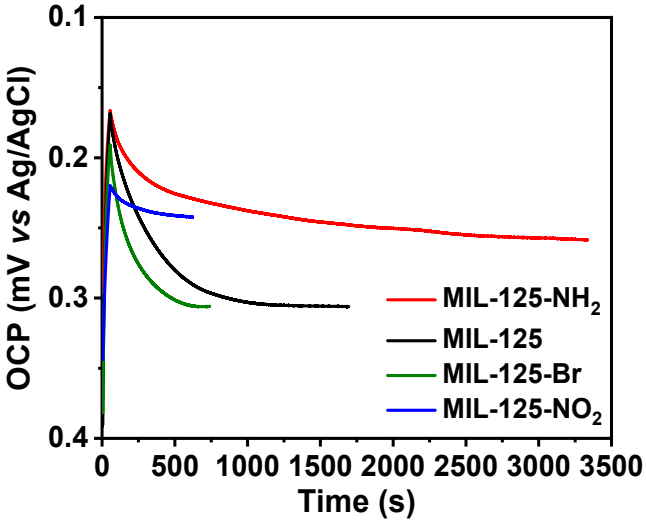

Fig. S19 The open-circuit potential (OCP) responses of MIL-125 and MIL-125-X (X = NH_2, NO_2, Br).

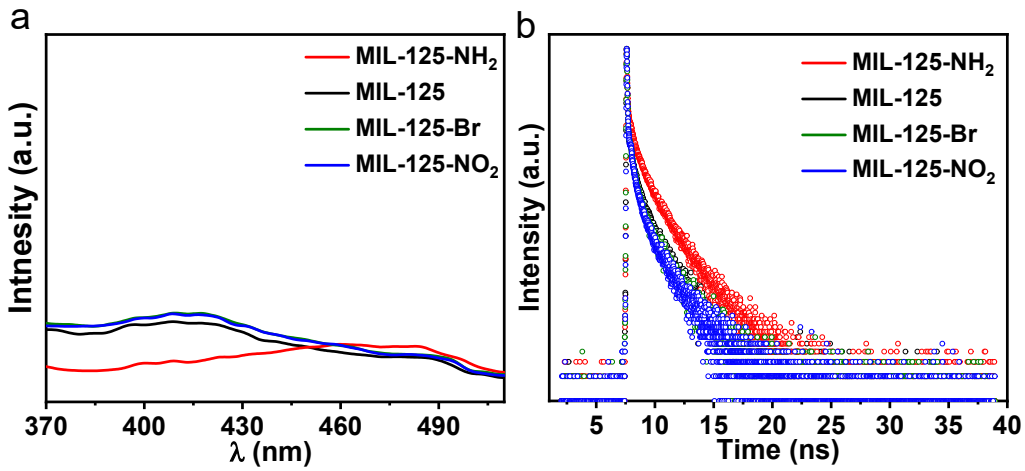

Fig. S20 (a) Steady-state and (b) Time-resolved PL spectra for MIL-125 and MIL-125-X (X = NH_2, NO_2, Br) in MeCN with TEOA as sacrificial agent. The fitted PL lifetime for MIL-125, MIL-125-NH_2, MIL-125-Br and MIL-125-NO_2 are 10.1 ps, 26.1 ps, 8.8 ps and 1.5 ps, respectively.

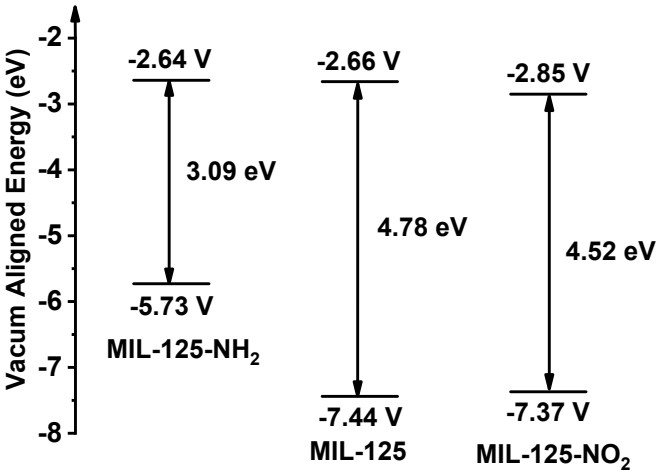

Fig. S21 The calculation of HOMO/LUCO energy levels of MIL-125-NH_2, MIL-125 and MIL-125-NO_2.

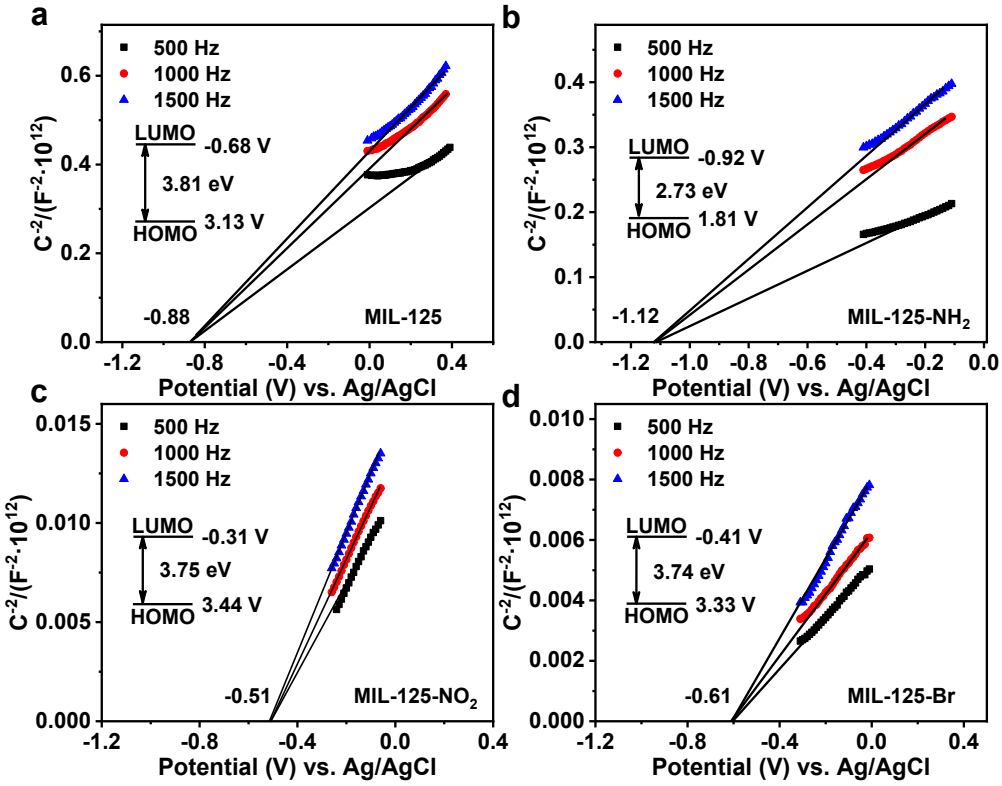

Fig. S22 Mott Schottky plots of MIL-125 and MIL-125-X (X = NH_2, NO_2, Br). Inset: the energy level position.

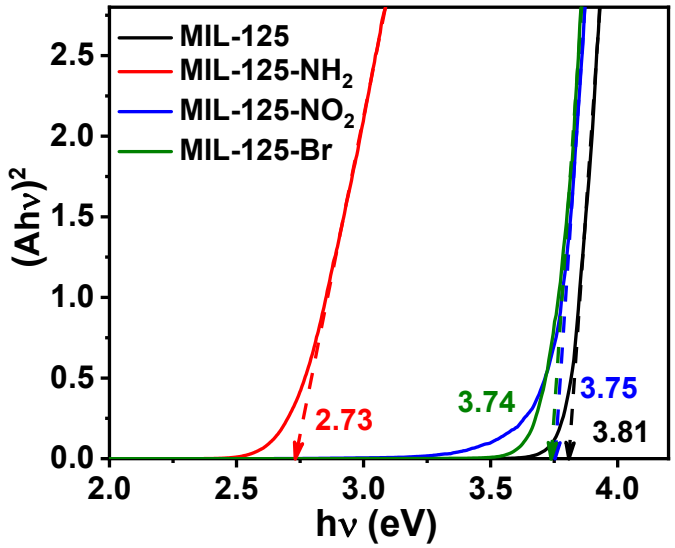

Fig. S23 The plots of transformed Kubelka-Munk function *vs*. the light absorption energy of MIL-125 and MIL-125-X (X = NH_2, NO_2, Br).

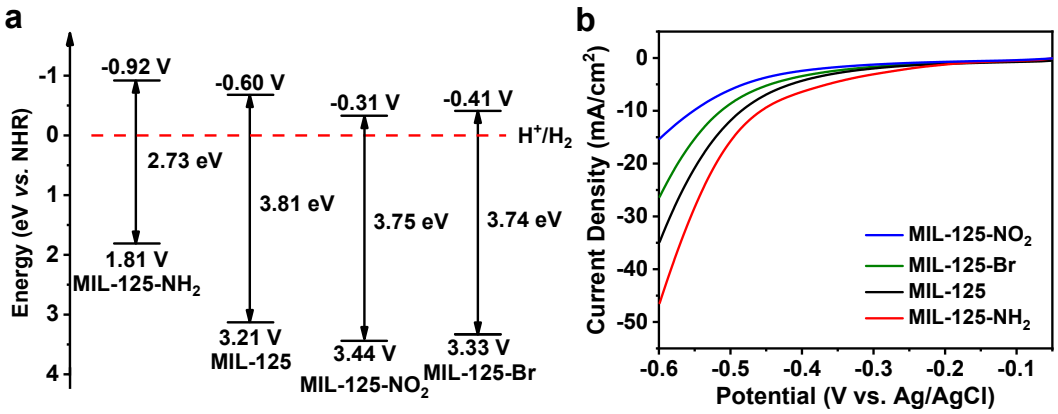

Fig. S24 (a) The band structure potential positions and (b) LSV curves for MIL-125 and MIL-125-X (X = NH_2, NO_2, Br).

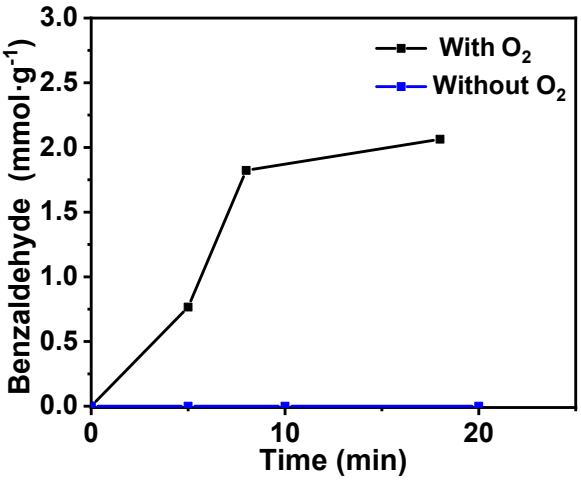

Fig. S25 The dark photocatalytic benzyl alcohol oxidation over MIL-125. Reaction conditions: 10 mg MIL-125 was dispersed in the solution of 0.5 ml benzyl alcohol and 3.5 ml anhydrous MeCN.

MIL-125 achieves a significantly higher dark photocatalytic benzyl alcohol oxidation activity with the assistance of O_2 than that without O_2 (negligible activity), indicating the process might be related to $O_2^{\bullet-}$-involved oxidation mechanism.

Table S1. The zeta potential of Pt NPs and MIL-125 and MIL-125-X (X = NH_2, NO_2, Br).

Cat	Zeta potential (mV)
Pt NPs	1.30
MIL-125	-26.5
MIL-125-NH_2	-43.4
MIL-125-Br	-37.4
MIL-125-NO_2	-38.3

There is an electrostatic interaction between Pt NPs and MOF due to the opposite of the zeta potentials of them.

Table S2. The lifetimes extracted from time-resolved PL spectra in MeCN.

Cat	lifetime
MIL-125	55.29 ps
MIL-125-NH_2	624.13 ns
MIL-125-Br	37.61 ps
MIL-125-NO_2	31.21 ps

Table S3. The estimated percentage of excited and converted Ti^{3+} in MIL-125-NH_2.

	Mmol
consumed TEOA	4.3
total Ti species in MIL-125-NH_2	49.2
the released electrons by Ti^{3+} for H_2 production	2.4

Reaction condition: 10 mg MIL-125-NH_2, 3.5 mL MeCN, 0.5 mL TEOA as a sacrificial agent, 0.25 mL Pt NPs solution (0.5 mg/mL) as co-catalyst, 25°C, ALM

Ideally, the theoretical ratio of consumed TEOA and hole is 1:1; the theoretical ratio of electron and hole is also 1:1. Therefore, the amount of Ti^{3+} generated in the light harvesting step can be deduced by the consumed TEOA; the "useful" Ti^{3+} for H_2 production in the dark can be evaluated based on measured H_2 amount.

The consumed TEOA amount is measured to be 4.3 μmol by GC with a FID detector, from which the total Ti^{3+} excited in the light harvesting step is calculated to be 8.6%, according to the total 49.2 μmol Ti^{4+} in MIL-125-NH_2. On the other hand, the generated H_2 amount in the dark is 1.2 μmol, and the released electrons by Ti^{3+} for H_2 production is 2.4 μmol, from which the "useful" Ti^{3+} for H_2 production, relative to the total Ti^{3+}, is 55.3%.

References

S1. R. Liang, R. Huang, X. Wang, S. Ying, G. Yan, and L. Wu, *Appl. Surf. Sci.,* 2019, **464**, 396-403.

S2. P. Liu, Y. Zhao, R. Qin, S. Mo, G. Chen, L. Gu, D. M. Chevrier, P. Zhang, Q. Guo, D. Zang, B. Wu, G. Fu and N. Zheng, *Science*, 2016, **352**, 797-800.